ORIGINAL ARTICLE

Journal of Cachexia, Sarcopenia and Muscle 2017; **8**: 974–990
Published online 3 July 2017 in Wiley Online Library (wileyonlinelibrary.com) **DOI:** 10.1002/jcsm.12222

Obestatin controls the ubiquitin–proteasome and autophagy–lysosome systems in glucocorticoid-induced muscle cell atrophy

Tania Cid-Díaz[1], Icía Santos-Zas[1], Jessica González-Sánchez[1], Uxía Gurriarán-Rodríguez[2], Carlos S. Mosteiro[1], Xesús Casabiell[3], Tomás García-Caballero[4], Vincent Mouly[5], Yolanda Pazos[1] & Jesús P. Camiña[1]*

[1]*Área de Endocrinología Molecular y Celular, Instituto de Investigación Sanitaria de Santiago (IDIS), Complejo Hospitalario Universitario de Santiago (CHUS), Servicio Gallego de Salud (SERGAS), Choupana s/n, 15706, Santiago de Compostela, Spain;* [2]*Sprott Center for Stem Cell Research, Ottawa Hospital Research Institute, 501 Smyth Road, Ottawa, Ontario K1H 8L6, Canada;* [3]*Departamento de Fisiología, Facultad de Veterinaria, Universidad de Santiago de Compostela (USC), Carballo Calero s/n, 27002, Lugo, Spain;* [4]*Departamento de Ciencias Morfológicas, Facultad de Medicina, USC, San Francisco s/n, 15704, Santiago de Compostela, Spain;* [5]*Sorbonne Universités, UPMC Université Paris 06, INSERM UMRS974, CNRS FRE3617, Center for Research in Myology, 47 Boulevard de l'hôpital, 75013, Paris, France*

Abstract

Background Many pathological states characterized by muscle atrophy are associated with an increase in circulating glucocorticoids and poor patient prognosis, making it an important target for treatment. The development of treatments for glucocorticoid-induced and wasting disorder-related skeletal muscle atrophy should be designed based on how the particular transcriptional program is orchestrated and how the balance of muscle protein synthesis and degradation is deregulated. Here, we investigated whether the obestatin/GPR39 system, an autocrine/paracrine signaling system acting on myogenesis and with anabolic effects on the skeletal muscle, could protect against glucocorticoid-induced muscle cell atrophy.
Methods In the present study, we have utilized mouse C2C12 myotube cultures to examine whether the obestatin/GPR39 signaling pathways can affect the atrophy induced by the synthetic glucocorticoid dexamethasone. We have extended these findings to *in vitro* effects on human atrophy using human KM155C25 myotubes.
Results The activation of the obestatin/GPR39 system protects from glucocorticoid-induced atrophy by regulation of Akt, PKD/PKCμ, CAMKII and AMPK signaling and its downstream targets in the control of protein synthesis, ubiquitin–proteasome system and autophagy–lysosome system in mouse cells. We compared mouse and human myotube cells in their response to glucocorticoid and identified differences in both the triggering of the atrophic program and the response to obestatin stimulation. Notably, we demonstrate that specific patterns of post-translational modifications of FoxO4 and FoxO1 play a key role in directing FoxO activity in response to obestatin in human myotubes.
Conclusions Our findings emphasize the function of the obestatin/GPR39 system in coordinating a variety of pathways involved in the regulation of protein degradation during catabolic conditions.

Keywords Skeletal muscle; Skeletal muscle cell atrophy; Skeletal muscle atrophy; Obestatin signalling

Received: 30 December 2016; Revised: 9 April 2017; Accepted: 22 May 2017
**Correspondence to: Jesus P. Camiña, PhD, Laboratorio de Endocrinología Celular, IDIS, Hospital Clínico Universitario de Santiago, Trav. Choupana, s/n. 15706 Santiago de Compostela, Spain. Tel.: 0034981955072, Email: jesus.perez@usc.es*

Introduction

The control of muscle mass is determined by an active balance between anabolic and catabolic processes.[1–3] A crucial component of the anabolic machinery for protein synthesis is the mammalian target of rapamycin complex 1 (mTORC1).[4] Mammalian target of rapamycin complex 1, which includes three essential and evolutionarily conserved core subunits (mTOR, Raptor and mLST8), is responsive to both organismal and cellular nutritional status, and controls downstream metabolic processes. Mammalian target of rapamycin complex 1 activation leads to both an acute increase in the

© 2017 The Authors. Journal of Cachexia, Sarcopenia and Muscle published by John Wiley & Sons Ltd on behalf of the Society on Sarcopenia, Cachexia and Wasting Disorders
This is an open access article under the terms of the Creative Commons Attribution-NonCommercial License, which permits use, distribution and reproduction in any medium, provided the original work is properly cited and is not used for commercial purposes.

translation of specific mRNAs and a broader increase in the protein synthesis capacity of the cell. mTORC1 regulates 5-cap-dependent mRNA translation through two sets of direct downstream targets: the eukaryotic initiation factor 4E (eIF4E)-binding proteins (4E-BP1 and 2) and the ribosomal S6 kinases (S6K1 and 2). 4E-BPs appear to have the most profound effect on mRNA translation downstream of mTORC1, binding to eIF4E at the 5-cap of mRNAs and blocking assembly of the translation initiation complex. The phosphorylation of 4E-BP1 and 2 by mTORC1 stimulates their release from eIF4E, allowing translation initiation to proceed. Systemic changes in the metabolism of the organism are sensed by mTORC1 through pathways activated by secreted growth factors, cytokines and hormones: mTORC1 is activated by insulin and most other growth factors through either receptor tyrosine kinases (RTKs) or G-protein-coupled receptors (GPCRs) at the cell surface. Downstream of these receptors, two major signalling pathways are involved in mTORC1 activation: the Akt and Erk1/2 pathways. Activation of mTORC1 is also dependent on sufficient levels of essential intracellular nutrients, including amino acids, glucose and oxygen. Protein degradation in skeletal muscle cells is essentially mediated by the activity of two conserved pathways: the ubiquitin–proteasome pathway and the autophagic/lysosomal pathway.[5] Both systems are coordinately regulated to remove proteins and organelles in atrophying cells.[6,7] The ubiquitin–proteasome pathway is responsible for the turnover of the majority of soluble and myofibrillar muscle proteins by the transcriptional activation of a set of E3 ligase-encoding genes, e.g. muscle RING-finger 1 (MuRF1) and atrogin-1/MAFbx.[8,9] Autophagy also plays an important role in the degradation of skeletal muscle as a consequence of an ordered transcriptional program involving a battery of genes, e.g. LC3, p62 and Bnip3.[10] Both autophagy–lysosome and ubiquitin–proteasome systems are transcriptionally controlled through the expression of a particular gene set: Forkhead box class O factors (FoxOs).[11] Members of the FoxO family (FoxO1, 3, 4 and 6) were identified as the main transcription factors regulating MAFbx expression.[9] Importantly, FoxO3 regulates autophagy coordinating the proteasomal dependent removal of proteins with the autophagy-dependent clearance of organelles.[6,12] The use of FoxO1 knockout mice has demonstrated a role for this factor in muscle protein homeostasis showing partial protection from muscle loss during chronic kidney disease.[13] FoxO1 deficiency was associated with partial reduction in the expression of MAFbx, MuRF1 and the lysosomal enzyme, Cathepsin-L.[13,14] Recent findings underscore the central function of FoxOs in coordinating a variety of stress-response genes during catabolic conditions.[15] It is evident that each atrophic phenotype involves specific signalling pathways; some triggering FoxOs, and that other components of the cellular machinery can participate in the progression of atrophy.[16] These positive and negative pathways are balanced in a highly coordinated manner for the maintenance of muscle homeostasis, myofibre size and total muscle volume.[1]

The actions of adrenal glucocorticoids are mediated by a signalling pathway involving the ubiquitously expressed glucocorticoid receptor (GR), a prototypic member of the nuclear receptor superfamily, which acts as a ligand-dependent transcription factor.[17] In skeletal muscle, glucocorticoids elicit a variety of biological actions in the metabolism of glucose, lipids and proteins and contribute to metabolic homeostasis.[18] A prolonged oversecretion or exogenous administration of glucocorticoid leads to many pathological conditions characterized by muscle atrophy, e.g. sepsis, cachexia, starvation, metabolic acidosis and severe insulinopenia, associated with an increase in circulating glucocorticoid levels.[18–21] Normally, glucocorticoid-induced muscle atrophy is characterized by fast-twitch type II glycolytic muscle fibre loss with reduced or no impact on type I fibres. Previous reports suggested the implication of the catabolic processes through the induction of a set of genes including the E3 ubiquitin ligases MAFbx, MuRF1 and myostatin.[19,20] The involvement of FoxO transcription factors is reported in the gene regulation of MAFbx and MuRF1 in the presence of an excess of glucocorticoids.[9,22] Furthermore, the identification of target genes of the GR in skeletal muscle, i.e. REDD1 and KLF15, involved in the regulation of the expression of MAFbx and MuRF1 genes, demonstrated the implication of GR in a variety of downstream molecular cascades leading to muscle atrophy.[23] Notably, a mutually crosstalk between GR and mTOR suggests a coordinated interaction between the catabolic signal and the anabolic machinery.[23]

The development of strategies to counteract glucocorticoid- and disease-induced skeletal muscle atrophy should be addressed on the bases on how the particular transcriptional program is orchestrated and how the balance of muscle protein synthesis and degradation might be deregulated. Previously, we demonstrated that the obestatin/GPR39 system exerts an autocrine function to control the myogenic program through regulation of the different stages involved in myogenesis: proliferation, migration, fusion and myofibre growth.[24,25] Obestatin/GPR39 signalling leads to an induction of the Akt/mTOR anabolic growth pathway, exerting a role on protein synthesis and leading to increases in muscle size.[24–26] Recent findings unveil a molecular mechanism whereby the ß-arrestins function as a link between GPR39 and the epidermal growth factor receptor (EGFR) to regulate specific steps of the myogenic process. Obestatin-induced mitogenic action is mediated by ERK1/2 and JunD activity, in a G-dependent mechanism. At a later stage of myogenesis, scaffolding proteins β-arrestins are essential for the activation of cell cycle exit and differentiation through the EGFR transactivation. This signalplex regulates the mitotic arrest by p21 and p57 expression and mid to late stages of

differentiation through JNK/c-jun, CAMKII, Akt and p38 pathways.[26]

Based on the anabolic action of the obestatin/GPR39 system, we hypothesized that this system counteracts the catabolic processes provoked by glucocorticoids. To that end, mouse C2C12 myotubes were treated with dexamethasone, as *in vitro* model of skeletal muscle cell atrophy.[9,22,27,28] We investigated the cross-talk between protein degradation and synthesis and provide evidence that the obestatin/GPR39 system acts through the Akt/FoxO axis to control proteasome- and autophagy-related factors. To examine if these pathways were also operative in human, we studied how this catabolic condition was reversed by the obestatin/GPR39 system in human myotubes (primary and immortalized myogenic cells). We provided evidence *in vitro* that obestatin triggers an antiatrophic signalling pathway, thereby protecting from experimentally induced atrophy. Surprisingly, we also found key differences in the execution of the atrophic program and in the response to obestatin stimulation between murine and human muscle cells. These data suggest that such differences should be taken into account when designing drug development and clinical translation to counteract atrophy.

Materials and methods

Materials

Mouse/rat obestatin was obtained from California Peptide Research (Napa, CA, USA). Antibodies used are listed in Table S1. All other chemical reagents were from Sigma Chemical Co. (St. Louis, MO, US).

Cell culture and differentiation

Mouse C2C12 (ECACC, Whiltshire, UK) myoblasts were cultured as described by the supplier (ECACC, Whiltshire, UK). Briefly, C2C12 myoblasts were maintained in growth medium (GM) containing DMEM supplemented with 10% foetal bovine serum (FBS), 100 U/mL penicillin and 100 U/mL streptomycin. For routine differentiation, the cells were grown to ~80% confluence, and GM was replaced with differentiation medium (DM; DMEM supplemented with 2% horse serum (HS), 100 U/mL penicillin and 100 U/mL streptomycin) for 7 days unless otherwise stated.

Myogenic primary, C25 cells and clonal line, KM155C25 Clone 48 (KM155C25 cells), were obtained from the platform for immortalization of human myoblasts of the Center for Research in Myology in Paris (Paris, France), who developed the isolation and immortalization from a biopsy obtained through MYOBANK, a partner in the EU network EuroBioBank (gracilis muscle, donor age 25 years). Primary myogenic cells isolated from biopsie were purified by magnetic activated cell sorting using anti-CD56 (a specific marker of myoblasts) beads (MACS, Miltenyl Biotech). Purity before and after cell sorting was determined by immunolabelling (anti-desmin and anti-mouse IgG1 AlexaFluor 488 antibodies) following the protocols previously described (29). Myogenic primary line (C25 cells) were cultured in GM containing Medium 199:DMEM (1:4, v/v; Lonza, Pontevedra, SP) supplemented with 20% FBS (v/v), 50 μg/mL gentamicin (Invitrogen), 25 μg/μL fetuin, 5 ng/mL hEGF, 0.5 ng/mL bFGF and 50 μg/mL gentamycin (Invitrogen). Differentiation into myotubes was initiated by switching to DM [DMEM supplemented with 50 μg/mL gentamycin (Invitrogen)] on gelatin from porcine skin-covered (Sigma-Aldrich, MO, USA) multiwell for 7 days unless otherwise stated.

Stable immortalized cell line from C25 cells was carried out as previously described (29). In brief, primary C25 cells were co-transduced with two retroviral vectors expressing hTERT and CDK-4 cDNA.[29] Co-transduced cells were selected by neomycin and puromycin and then purified using magnetic beads coupled to antibodies directed against the myogenic marker CD56. Following culture at clonal density, individual myogenic clones with extended proliferative lifespans, as compared with the untranduced cells, were isolated from each population. Immortalized human myoblasts, KM155C25 Clone 48 (KM155C25 cells), maintain their capacity to differentiate both *in vitro* and *in vivo* after transplantation into the regenerating muscles of immunodeficient mice.[29,30] KM155C25 cells were cultivated in GM containing Medium 199:DMEM (1:4, v/v; Lonza, Pontevedra, SP) supplemented with 20% FBS (v/v), 25 μg/μL fetuin, 5 ng/mL hEGF, 0.5 ng/mL bFGF and 50 μg/mL gentamycin (Invitrogen) as described previously.[26,29] Differentiation into myotubes was initiated at 90% confluence by switching to DM [DMEM supplemented with 50 μg/mL gentamycin (Invitrogen)] for 7 days unless otherwise stated.

Murine or human myotubes were treated with dexamethasone (Dexa; 0.05–100 μM) for 24 h in the presence or absence of obestatin (5–100 nM), or with insulin (100 nM) as a positive control of atrophy protection.

Immunofluorescence

Myoblast cells were cultured on multiwells and differentiated into myotubes for 7 days. Myotubes were then treated with Dexa for 24 h in the presence or absence of obestatin or insulin as indicated above. Cells were fixed with 96% ethanol, washed with ice cold PBS, permeabilized with PBST (0.3% Triton X-100, 0.1 M glycine in PBS), blocked with 1% BSA in PBST and then incubated with primary antibody diluted in 1% BSA in PBST at 4°C. After three washes with PBS, cells were incubated with the secondary antibody (FITC-conjugate

goat anti-mouse antibody or FICT-conjugated goat anti-rabbit antibody) diluted in 1% BSA in PBST (1:1000) at room temperature and then washed with ice cold PBS. Topro or DAPI was used to counterstain the cell nuclei (Invitrogen). Digital images of cell cultures were acquired with a Leica TCS-SP5 spectral confocal microscope (Leica Microsystems, Heidelberg, Germany). Myotube areas (MHC^+ cells, $\geq$ 3 nuclei) were quantified by measuring a total of $>$100 myotube areas from five random fields in three replicate using ImageJ64 analysis software.

Small interfering RNA (siRNA) silencing of gene expression

Chemically synthesized double-stranded siRNA duplexes targeting FoxO4, β-arrestin 1 or β-arrestin 2 were selected from ON-TARGETplus SMARTpool siRNA from Thermo Fisher Scientific (Dharmacon; human FoxO4: AGUCAUGCCUGGAA GCUUU, GAGAAGCGACUGACACUUG, GGAAAUACCAGCUUCA GUC, CAACGAGGCCACCGGCAAA; human β-Arrestin 1: UGGA UAAGGAGAUCUAUUA, AUGGAAAGCUCACCGUCUA, GAACUG CCCUUCACCCUAA, GAACGAGACGCCAGUAGAU; human β-Arrestin 2: CGAACAAGAUGACCAGGUA, CGGCGUAGACUUUG AGAUU, GGGCUUGUCCUUCCGCAAA, UAGAUCACCUGGACAA AGU). An ON-TARGETplus nontargeting siRNA was used as a control for all siRNA experiments. Human KM155C25 myotubes were transfected at day-6 post-differentiation with Lipofectamine 2000 (Invitrogen), following manufacturer's instructions.

SDS-PAGE and western blot analysis

The cell samples were directly lysed in ice-cold RIPA buffer [50 mM Tris–HCl (pH 7.2), 150 mM NaCl, 1 mM EDTA, 1% (v/v) NP-40, 0.25% (w/v) Na-deoxycholate, protease inhibitor cocktail (Sigma Chemical Co, St. Louis, MO, US), phosphatase inhibitor cocktail (Sigma Chemical Co, St. Louis, MO, US)]. The lysates were clarified by centrifugation (14 000 *g* for 15 min at 4°C), and the protein concentration was quantified using the QuantiPro™ BCA assay kit (Sigma Chemical Co, St. Louis, MO, USA). For immunoblotting, equal amounts of protein were fractionated by SDS-PAGE and transferred onto nitrocellulose membranes. Immunoreactive bands were detected by enhanced chemiluminescence (Pierce ECL Western Blotting Substrate; Thermo Fisher Scientific, Pierce, Rockford, IL, US).

Co-immunoprecipitation assays

Following treatment [DM, DM + Dexa (1 μM, 24 h), DM + Dexa (1 μM, 24 h) + obestatin (10 nM, 24 h)], KM155C25 myotubes cells were washed twice with ice-cold PBS and lysed in co-immunoprecipitation lysis buffer (50 mM Tris, 100 mM NaCl, 5 mM EDTA, 50 mM NaF, 1% Triton X-100, 10 mM glycerol phosphate, 200 μM sodium orthovanadate, 2.5 mM sodium pyrophosphate plus protease inhibitors). FoxO1 was immunoprecipitated using rabbit anti-FoxO1 antibody coupled to protein A-Dynabeads according to instruction provided by manufacturer (Thermo Fisher Scientific, Life Technology, Rockford, IL, US). The washed immunoprecipitates were subjected to western blot analysis using the indicated antibodies.

Protein synthesis assays

Protein synthesis was measured in C2C12 and KM155C25 myotubes using Click-iT®Plus OPP Protein Synthesis Assay (Thermo Fisher Scientific, Life Technology, Rockford, IL, USA). Murine or human myotubes were treated with Dexa (1 μM) in the presence or absence of obestatin (10 nM), or with obestatin (10 nM) in the presence or absence the protein synthesis inhibitor, cycloheximide (100 μM) for 24 h. Myotubes were then incubated with 20 μM Click-iT OPP in cell culture medium for 30 min at 37°C. The cells were washed with PBS and fixed with ethanol and permeabilized by 0.5% Triton X-100. Click-iT reaction was carried out according to manufacturer's instructions. HCS NuclearMask™Blue Stain was used to nuclei counterstain. Protein synthesis was measured as the mean intensity of the fluorescent signal and normalized to cell number assessed by the blue NuclearMask signal.

Data analysis

All values are presented as mean ± standard error of the mean (SEM). A Shapiro–Wilks normality test was performed for each data set. *T*-tests were carried out for comparisons between two samples. Unpaired *T*-test was used to assess the statistical significance of one-way or two-way analysis when the test statistic followed a normal distribution. $P < 0.05$ was considered as statistically significant (*,# $P < 0.05$).

Results

The obestatin/GPR39 system regulates the interplay between Akt and FoxO signalling in dexamethasone-induced atrophy in C2C12 myotubes

We first defined a dose–response effect for the synthetic glucocorticoid dexamethasone (Dexa, 0.05–100 μM) on MuRF1 and MAFbx protein content in fully differentiated C2C12 myotubes. After 24 h of Dexa treatment, a maximal

effect on MuRF1 and MAFbx protein content was detected at 1 μM Dexa [~4.5–4.9-fold, respectively (*Figure* 1A)], a concentration that was used for the subsequent assays. Upon these conditions, myotubes showed a 40 ± 2% decrease in area (*Figure* 1B). These changes were reversed by obestatin as revealed by a marked rescue of myotube area for the range of obestatin concentrations tested (5, 25 and 100 nM: 39 ± 2%, 36 ± 4% and 36 ± 2% increase over Dexa-treated myotubes, respectively; *Figure* 1B).[26] It should be noted that the myotube areas were ~27% larger in obestatin-treated cells as compared with insulin-treated cells (12 ± 3% increase over Dexa-treated myotubes; *Figure* 1B), used as positive control. A detailed area analysis at 5 nM obestatin revealed a significant increase, as compared with Dexa-treated myotubes, in the percentage of myotubes of larger area (*Figure* 1C): ~91% vs. 4% of myotubes in a range between 2×10^3–8×10^2 μm^2, and ~9% vs. 96% in the range between 8 and 2×10^2 μm^2, respectively.

At the molecular level, obestatin treatment (5–100 nM, 24 h) decreased the expression of the ubiquitin E3-ligases MuRF1 and MAFbx in Dexa-treated cells by 45–69% and 44–58%, respectively. Insulin (100 nM, 24 h) similarly decreased the MuRF1 and MAFbx expression by 62 ± 2% and 93 ± 2%, respectively (*Figure* 2A). It is important to highlight that the obestatin-activated signalling resulted in a strong up-regulation of myosin heavy chain (MHC) expression, showing levels 32–108% above those reached in Dexa-treated C2C12 myotubes (*Figure* 2A). The results achieved for MHC in response to obestatin (100 nM) were superior to those reached with insulin (108 ± 6% vs. 35 ± 3%, respectively). Furthermore, the muscle-specific transcription factor myogenin was up-regulated following Dexa treatment consistent with a role in the expression of the MuRF1 and MAFbx.[16] This up-regulation was increased by ~24% in obestatin- or insulin-treated C2C12 myotubes (*Figure* 2A). The down-regulation of ubiquitin E3-ligases and up-regulation of protein synthesis suggested the implication of the growth promoting obestatin/Akt–mTOR signalling pathway. Indeed, Akt activation, detected by the phosphorylation of its regulatory residue S473 [pAkt(S473)], was increased by 2.5- to 3.8-fold in obestatin-stimulated cells as compared with Dexa-treated C2C12 myotubes. The up-regulation of Akt activity was concomitant with a 2.6- to 2.8-fold increase in mTOR phosphorylation at S2448 [pmTOR(S2448) related to Dexa-treated cells], a 1.8- to 2.9-fold increase in S6 K1 phosphorylation at S371 [pS6K1(S371) related to Dexa-treated cells; *Figure* 2A] and by a 2.5- to 2.6-fold increase in phosphorylation of its downstream target, the ribosomal protein S6 at S240/244 [pS6(S240/244); *Figure* 2B]. In insulin-treated cells, pmTOR(S2448), pS6K1(S371) and pS6(S240/244) were also significantly increased (1.8-, 1.9- and 2.5-fold, respectively). Furthermore, obestatin markedly promoted 4E-BP1 hyperphosphorylation at T70 [p4E-BP1(T70)], especially concerning the γ form (2.0- to 2.9-fold), altering the basal phosphorylation of β and γ forms at T37/T46 [p4E-BP1(T37/46); 1.3- to 1.6-fold and 2.0- to 2.9-fold, respectively] in Dexa-treated cells (*Figure* 2B). The p4E–BP1(T70) γ form was also increased by insulin (1.9-fold related to Dexa-treated cells) but insulin did not appreciably alter basal T37/T46 phosphorylation (β or γ forms). Obestatin treatment (10 nM, 24 h) increased protein synthesis in C2C12 myotubes by 79 ± 6% in Dexa-treated cells (*Figure* 2C).

One mechanism by which Akt reduces the expression of the ubiquitin E3-ligases is the phosphorylation and subsequent nuclear exclusion of FoxO family members. As shown in *Figure* 3A, obestatin markedly increased FoxO4 phosphorylation at T28 [pFoxO4(T28)] by 1.9- to 3.4-fold related to Dexa-treated C2C12 myotubes but did not change FoxO3a and FoxO1 phosphorylation (*Figure* 3A). In contrast, insulin treatment did appreciably increase phosphorylation of FoxO1 at T24 (3.8-fold related to Dexa-treated C2C12 myotubes) but had no effect at S256 (*Figure* 3A). Furthermore, insulin increased FoxO3a phosphorylation at T32 and S253 (2.2-and 3.2-fold, respectively) with minor effect on FoxO4 phosphorylation (1.4-fold; *Figure* 3A).

Because mTOR is a suppressor of the autophagy–lysosome system, while FoxO is an inducer of autophagy-dependent degradation, the status of this degradative process was checked in response to activation of the obestatin/GPR39 system. The levels of microtubule-associated protein 1 light chain 3 isoform I (LC3-I) did not change in Dexa-treated myotubes, whereas the lipidated form (LC3-II), a reliable marker of autophagosome formation, was significantly elevated (*Figure* 3B), as revealed by an increase in the LC3II/LC3I ratio observed in Dexa-treated C2C12 myotubes. This increase was reversed by 18–34% upon obestatin treatment consistent with decreased LC3-II levels (*Figure* 3B). Furthermore, the levels of p62 were assayed as a measure of substrate sequestration into autophagosomes: p62 binds LC3 and substrates marked for degradation by ubiquitylation. Significant accumulation of p62 protein was seen in obestatin-stimulated cells as compared with Dexa-treated C2C12 myotubes (144–169%) indicating a block in autophagy (*Figure* 3B). In contrast, obestatin stimulation was associated with a reduction in the expression of the lysosomal enzyme Cathepsin L by 31–29% as compared with Dexa-treated myotubes, further supporting an at least partial inactivation of autophagy. Insulin treatment decreased LC3-II/LC3-I ratio and increased p62 accumulation, although it failed to modify Cathepsin L levels (*Figure* 3B). Taken together, our data support a model where the interplay between Akt, mTOR and FoxO4 regulates two of the main proteolytic systems, the ubiquitin–proteasome and the autophagy–lysosome systems, and the signalling associated with protein translation in response to the obestatin/GPR39 system.

Figure 1 Activation of the obestatin/GPR39 system regulates the C2C12 myotube growth under Dexa-treatment. *(A)* Immunoblot analysis of Murf1 and MAFbx in C2C12 myotubes under Dexa-treatment (Dexa; 0.05–100 μM; 24 h). Immunoblots are representative of the mean value of three independent experiments. Data were expressed as mean ± SEM obtained from intensity scans. *(B) Left panel*, immunofluorescence detection of MHC in C2C12 myotube cells after stimulation under differentiation medium (DM), DM + Dexa (1 μM, 24 h), DM + Dexa (1 μM, 24 h) + obestatin (5–100 nM, 24 h) or DM + Dexa (1 μM, 24 h) + insulin (100 nM, 24 h) applied at day 7 post-differentiation. Topro was used to identify the cell nucleus. *Right panel* corresponds to myotube area (μm^2) assessment for the different treatments (n = 10 per group). Data were expressed as mean ± SEM. * $P < 0.05$ Dexa vs. control values (DM). *(C)* Myotube area and myotube number were measured and expressed as % of total myotube number for each group (n = 10 per group).

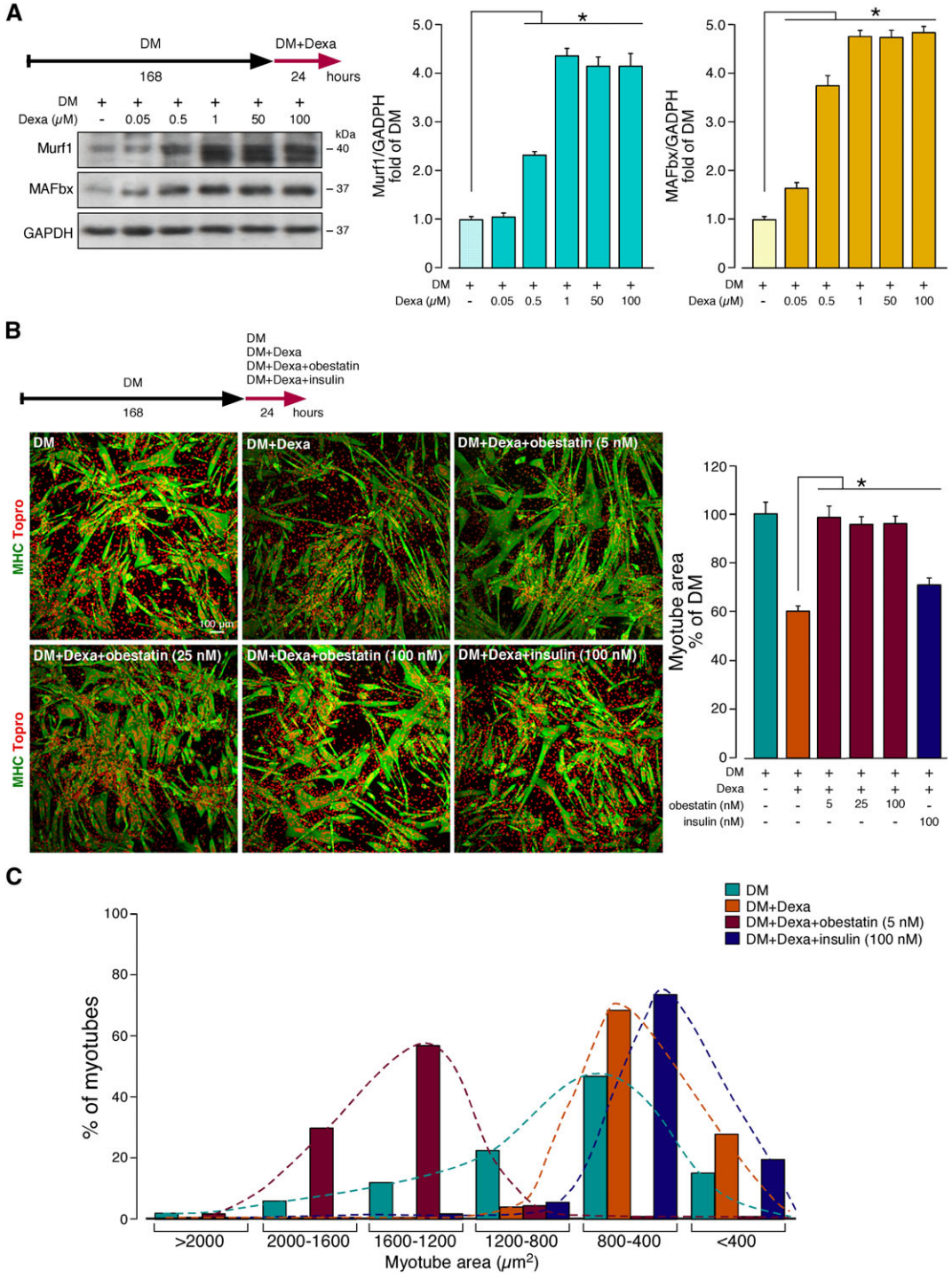

DOI: 10.1002/jcsm.12222

Figure 2 The obestatin/GPR39 system protects C2C12 myotubes from dexamethasone-induced atrophy with induction of protein synthesis. Immunoblot analysis of *(A)* Murf1, MAFbx, pAkt(S473), pmTOR(S2448), pS6K1(S6371), myogenin and MHC; and, *(B)* p4E-BP1(T70), p4E-BP1(T37/46) and pS6(S240/244), in myotube C2C12 cells under DM, DM + Dexa (1 μM, 24 h), DM + Dexa (1 μM, 24 h) + obestatin (5–100 nM, 24 h) or DM + Dexa (1 μM, 24 h) + insulin (100 nM, 24 h). In A and B, protein level was expressed as fold of control cells in DM (n = 5). Immunoblots are representative of the mean value. Data were expressed as mean ± SEM obtained from intensity scans. * $P < 0.05$ Dexa vs. DM and # $P < 0.05$ obestatin vs. Dexa. *(C)* Protein synthesis was measured in C2C12 myotubes treated with DM, DM + Dexa (1 μM, 24 h), DM + Dexa (1 μM, 24 h) + obestatin (10 nM, 24 h), DM + obestatin (10 nM, 24 h), DM + cycloheximide (100 μM) or DM + obestatin (10 nM, 24 h) + cycloheximide (100 μM), and data were expressed as fold of DM. Data were expressed as mean ± SEM (n = 3). * $P < 0.05$ Dexa, obestatin, cycloheximide or cycloheximide + obestatin vs. DM, and # $P < 0.05$ obestatin vs. Dexa or cycloheximide + obestatin.

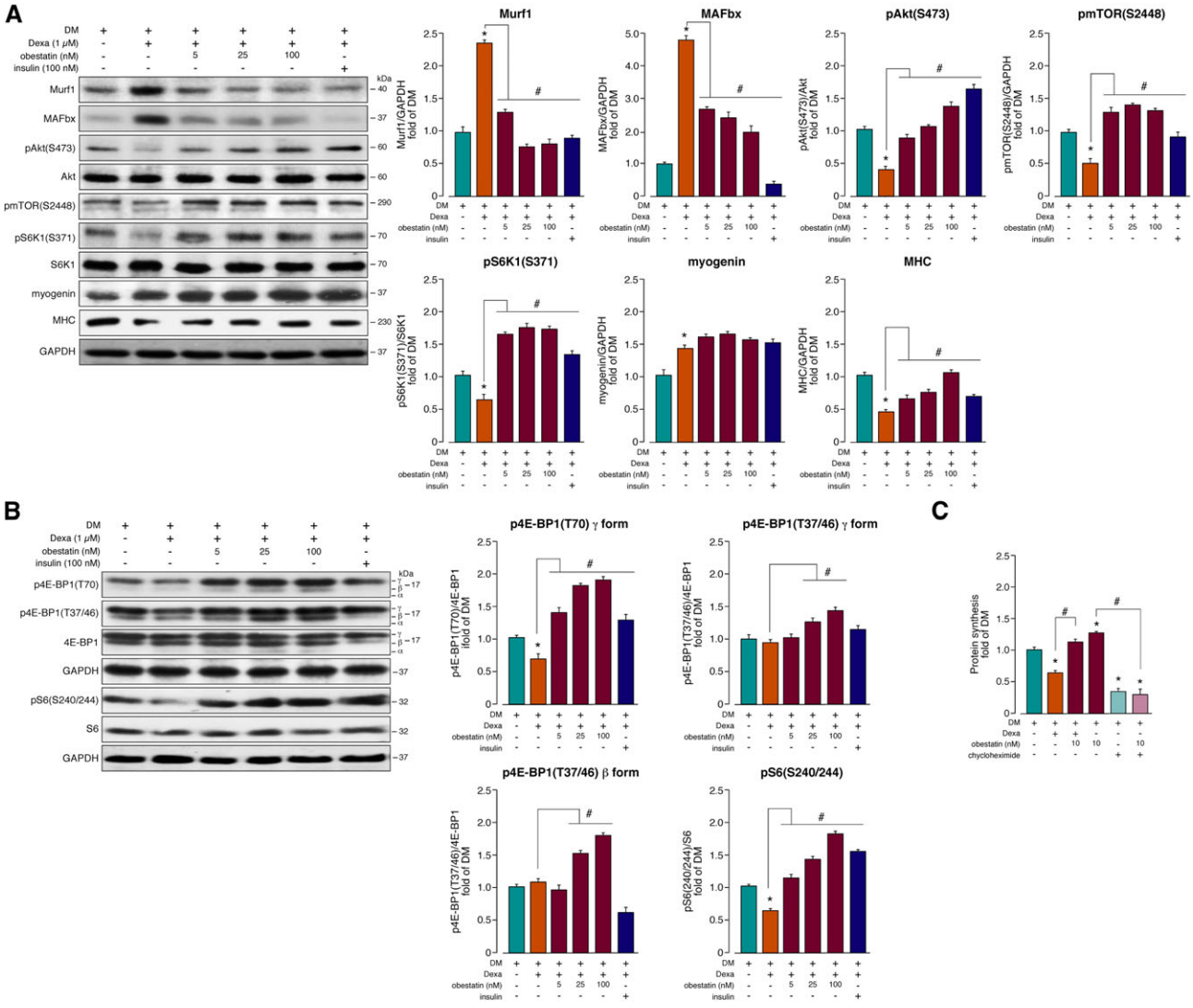

The obestatin/GPR39 system attenuates atrophy-related gene expression by targeting FoxO4 in dexamethasone-induced atrophy of human KM155C25 myotubes

In order to validate whether the obestatin/GPR39 signalling is conserved between human and mouse, we used an *in vitro* cell culture model of human skeletal muscle: the human muscle stem-cell line immortalized from a control individual, KM155C25 cells (for details see Methods). Treatment of this cell line with Dexa resulted in dose-dependent increases in the MuRF1 and MAFbx protein content with a maximal effect at 1 μM Dexa [5.4–5.9-fold, respectively (*Figure* 4A)]. Up-regulation of ubiquitin E3-ligases was concomitant with a decrease in Akt activity and MHC expression (*Figure* 4A). Intriguingly, myogenin expression was down-regulated following Dexa treatment, contrary to what was observed in C2C12 myotubes, possibly related to the fact that myogenin is up-regulated during the initial phases of differentiation,

DOI: 10.1002/jcsm.12222

Figure 3 Screening of intracellular targets associated to the activation of the obestatin/GPR39 system in Dexa-treated C2C12 myotubes. *(A)* Immunoblot analysis of the phosphorylation partner of FoxO3, FoxO1 and FoxO4 in myotube C2C12 cells under DM, DM + Dexa (1 μM, 24 h), DM + Dexa (1 μM, 24 h) + obestatin (5–100 nM, 24 h) or DM + Dexa (1 μM, 24 h) + insulin(100 nM, 24 h). *(B)* Immunoblot analysis of autophagy-related proteins LC3, p62 and Cathepsin L in myotube C2C12 cells under DM, DM + Dexa (1 μM, 24 h), DM + Dexa (1 μM, 24 h) + obestatin (5–100 nM, 24 h) or DM + Dexa (1 μM, 24 h) + insulin(100 nM, 24 h). In A–B, protein level was expressed as fold of control cells in DM (n = 5). Immunoblots are representative of the mean value. Data were expressed as mean ± SEM obtained from intensity scans. * $P < 0.05$ Dexa vs. DM and # $P < 0.05$ obestatin vs. Dexa.

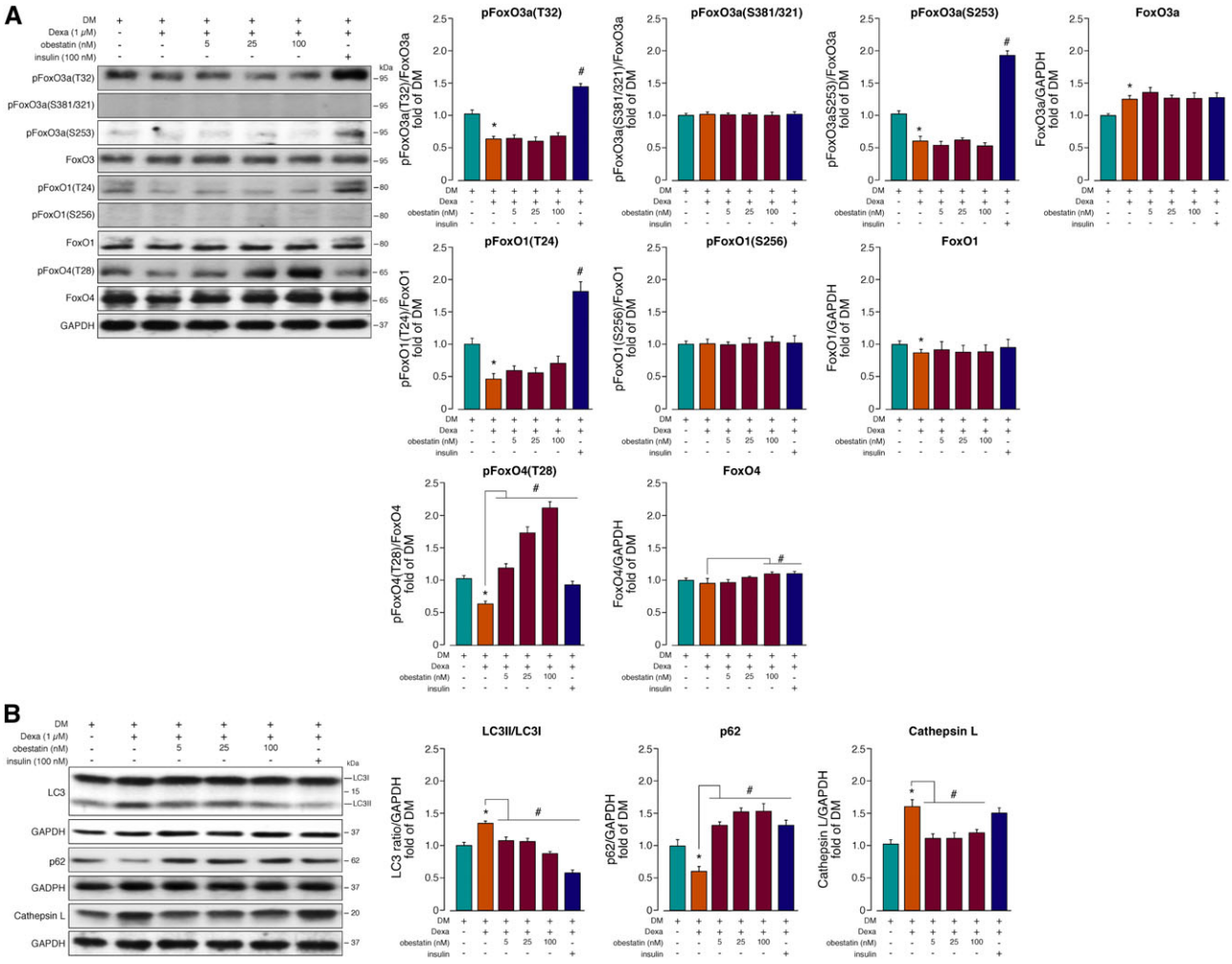

and the kinetics of differentiation may differ between C2C12 and KM155C25 (*Figure* 4A). An analysis of FoxO phosphorylation showed that Dexa markedly increased the basal level of FoxO3 phosphorylation at T32, S381 and S321. However, this effect was decreased at higher Dexa concentrations (*Figure* 4B). Unexpectedly, protein levels of FoxO3a were increased ~1.5-fold in response to Dexa (*Figure* 4B). In contrast, FoxO1 and FoxO4 phosphorylation had a tendency to decrease although not significantly (*Figure* 4B). Having evaluated the effect of Dexa under basal conditions, the action of obestatin/GPR39 signalling was determined on Dexa-treated myotubes at 1 μM concentration, based on the maximal effect on the MuRF1 and MAFbx expression at that dose. Obestatin treatment (10–100 nM, 24 h) decreased the expression of the ubiquitin E3-ligases MuRF1 and MAFbx by 65–80% and 35–42% in Dexa-treated cells, respectively. Insulin (100 nM, 24 h) similarly decreased the MuRF1 and MAFbx expression by 58 ± 2% and 18 ± 3%, respectively (*Figure* 4C). The obestatin-activated signalling caused up-regulation of MHC expression, showing levels 185–222% above those reached in Dexa-treated KM155C25 myotubes (*Figure* 4C). The results achieved for MHC were similar to those reached with insulin (192 ± 9% vs. 222 ± 5% for 100 nM obestatin). However, myogenin was not up-regulated following obestatin- or insulin-treated myotubes (*Figure* 4C). Under these conditions, obestatin treatment (10 nM, 24 h) increased protein synthesis by 91 ± 5% in Dexa-treated cells (*Figure* 4D). In addition, myotubes showed a decrease in area

DOI: 10.1002/jcsm.12222

Figure 4 The activation of obestatin/GPR39 system counteracts dexamethasone-induced atrophy in human KM155C25 myotubes. *(A)* Immunoblot analysis of Murf1, MAFbx, pAkt(S473), myogenin and MHC in KM155C25 myotubes under Dexa-treatment (Dexa; 0.05–100 μM; 24 h). *(B)* Immunoblot analysis of the phosphorylation partner of FoxO3, FoxO1 and FoxO4 in KM155C25 myotubes under Dexa-treatment (Dexa; 1–100 μM; 24 h). *(C)* Immunoblot analysis of Murf1, MAFbx, myogenin and MHC in KM155C25 myotubes under DM, DM + Dexa (1 μM, 24 h), DM + Dexa (1 μM, 24 h) + obestatin (10–100 nM, 24 h) or DM + Dexa (1 μM, 24 h) + insulin (100 nM, 24 h). *(D)* Protein synthesis was measured in KM155C25 myotubes treated with DM, DM + Dexa (1 μM, 24 h), DM + Dexa (1 μM, 24 h) + obestatin (10 nM, 24 h), DM + obestatin (10 nM, 24 h), DM + cycloheximide (100 μM) or DM + obestatin (10 nM, 24 h) + cycloheximide (100 μM), and data were expressed as fold of DM. Data were expressed as mean ± SEM (n = 3). * $P < 0.05$ Dexa, obestatin, cycloheximide or cycloheximide + obestatin vs. DM, and # $P < 0.05$ obestatin vs. Dexa or cycloheximide + obestatin. *(E) Left panel*, immunofluorescence detection of MHC in KM155C25 myotube cells under differentiation medium (DM), DM + Dexa (1 μM, 24 h), DM + Dexa (1 μM, 24 h) + obestatin (10 nM, 24 h) or DM + Dexa (1 μM, 24 h) + insulin (100 nM, 24 h) applied at day 7 post-differentiation. DAPI was used to identify the cell nucleus. *Right panel* corresponds to myotube area (μm^2) assessment for the different treatments (n = 10 per group). In A–C, immunoblots are representative of the mean value. Data were expressed as mean ± SEM obtained from intensity scans. * $P < 0.05$ Dexa vs. DM and # $P < 0.05$ obestatin vs. Dexa.

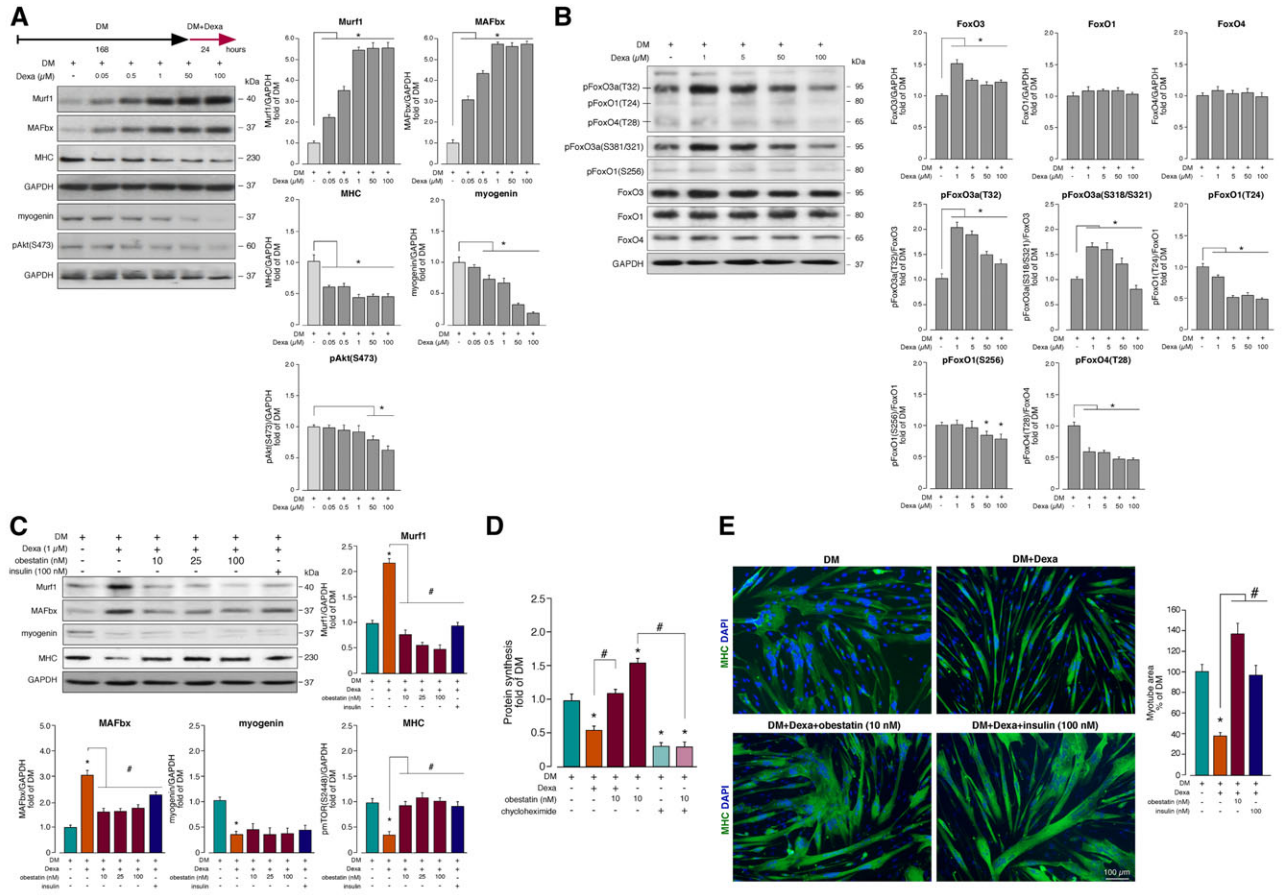

of 63 ± 3% in response to Dexa (*Figure* 4E). These changes were reversed by obestatin (10 nM, 24 h) as revealed by a marked increase in myotube area (~100 ± 12% over Dexa-treated myotubes, *Figure* 4E). Furthermore, the myotube areas were ~40% larger in the obestatin-treated cells than insulin-treated cells (60 ± 8% increase over Dexa-treated myotubes; *Figure* 4E), used as positive control. To assess how ubiquitin E3 ligases were regulated by obestatin/GPR39 signalling, the phosphorylation code of FoxO proteins was evaluated. As shown in *Figure* 5A, obestatin significantly increased the amount of phosphorylated FoxO4 at T28 and FoxO1 at S256 by 2.1- and 1.4-fold related to Dexa-treated KM155C25 myotubes, respectively. Obestatin stimulation failed to modify the phosphorylation levels of FoxO1 phosphorylation at T24. Interestingly, FoxO3 phosphorylation at T32, S381 and S321 sites was not modified by obestatin, but maintained at the Dexa-stimulated levels (*Figure* 5A). This activity was also tested on primary human myotubes obtained from C25 cells (for details see Methods). As shown in *Figure* S1, obestatin treatment not only reversed Dexa-induced myotube atrophy (*Figure* S1A) but also increased the amount of phosphorylated FoxO4 at T28 which correlated with decreased MuRF1 and MAFbx expression (*Figure* S1B).

DOI: 10.1002/jcsm.12222

Figure 5 Differential effect of obestatin/GPR39 signalling on FoxO phosphorylation and intracellular localization in human KM155C25 myotubes under dexamethasone treatment. *(A)* Immunoblot analysis of the phosphorylation partner of FoxO3, FoxO1 and FoxO4 in human KM155C25 myotubes under DM, DM + Dexa (1 μM, 24 h) or DM + Dexa (1 μM, 24 h) + obestatin (10–100 nM, 24 h). Immunoblots are representative of the mean value (n = 4). Data were expressed as mean ± SEM obtained from intensity scans. *(B) Upper panel*, immunofluorescence detection of FoxO1, FoxO3 and FoxO4 in KM155C25 myotube cells under differentiation medium (DM, control), DM + Dexa (1 μM, 24 h) or DM + Dexa (1 μM, 24 h) + obestatin (10 nM, 24 h) at day 7 post-differentiation. Cellular localization of the proteins was subsequently determined using fluorescence microscopy following fixation and incubation with DAPI to label cell nuclei. The mean fluorescence of FoxOs in nuclear and cytoplasmic compartments was calculated for each condition and was expressed as a ratio to indicate the relative localization (n = 10 per group). Data were expressed as mean ± SEM. * $P < 0.05$ Dexa vs. DM and # $P < 0.05$ obestatin vs. Dexa.

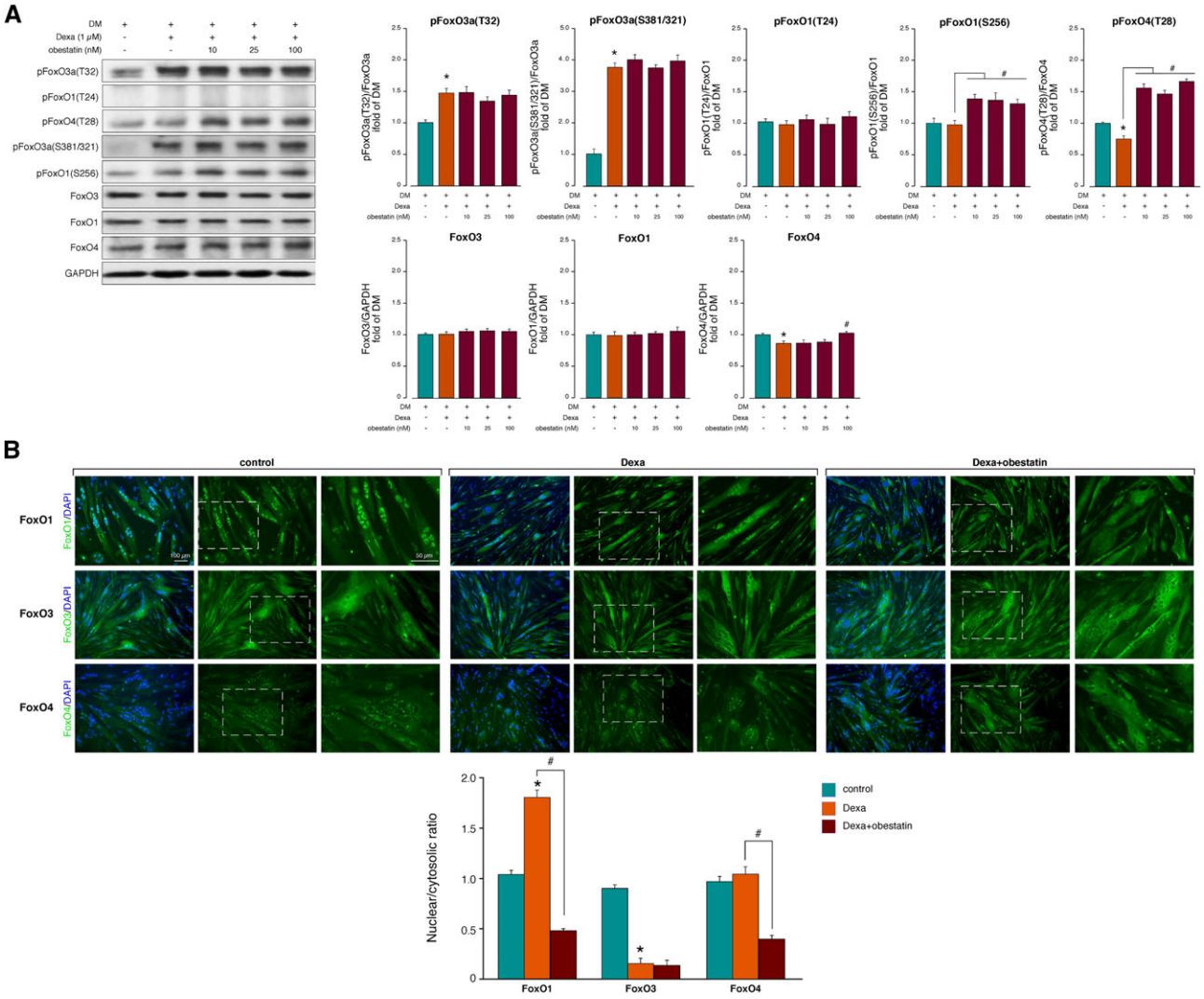

Having shown that obestatin induced negative regulation of FoxO transcription factors, we investigated the involvement of the β-arrestin signal complex.[26] The effect of down-regulation of β-arrestin 1 and β-arrestin 2 by specific siRNA was evaluated in KM155C25 myotubes. The siRNAs decreased β-arrestin 1 and β-arrestin 2 expressions by 58 ± 3 and 61 ± 4%, respectively (*Figure* S2). In these conditions, obestatin-stimulated phosphorylation of Akt, FoxO3a, FoxO4 and FoxO1 were reduced by depletion of β-arrestin 1 or 2 [pAkt(S473): 66 ± 1 or 72 ± 1%; pFoxO3a(T32): 68 ± 1 or 67 ± 3%; pFoxO4(T28): 78 ± 2 or 67 ± 2%; pFoxO1(T256): 47 ± 2 or 53 ± 3%; pFoxO3a(S318/321): 66 ± 2 or 63 ± 3%, respectively]. This finding provides a functional activity for β-arrestin-dependent signalplex being specific signalling arm to activate Akt/FoxO signalling in myotubes.

The localization of endogenous FoxO proteins was further visualized by fluorescence microscopy in KM155C25 myotubes, and the ratio of nuclear to cytoplasmic fluorescence was calculated (*Figure* 5B). As depicted in the

DOI: 10.1002/jcsm.12222

representative images, FoxO1, FoxO3a and FoxO4 were present both in the nucleus and in the cytoplasm in control conditions. FoxO1 was localized predominately to the nucleus in Dexa treated cells but showed increased localization to the cytoplasm in response to obestatin. FoxO3 was mainly localized in the cytoplasm in response to Dexa or obestatin (*Figure* 5B). FoxO4 localized in both the nucleus and cytoplasm in response to Dexa, but an increased cytoplasmic translocation was induced by obestatin (*Figure* 5B). Taken together, these results suggested that obestatin signalling induced FoxO4 T28 phosphorylation, inactivation and nuclear exclusion, contributing to the regulation of transcription of FoxO target genes, such as Murf1 and MAFbx. Indeed, siRNA experiments targeting FoxO4 (81 ± 4% reduction relative to si-control) significantly decreased the Murf1 and MAFbx expression in Dexa-stimulated cells by 55 ± 1 and 61 ± 1% relative to si-control, respectively (*Figure* 6A). Under these conditions, si-FoxO4 experiments increased the Murf1 and MAFbx expression in obestatin-stimulated cells by 88 ± 12 and 82 ± 6% relative to si-control, respectively. Furthermore, the FoxO4 knockdown showed deregulations of autophagy-related proteins. The acute FoxO4 deficiency on Dexa-treated cells increased the expression levels of p62 by 69 ± 3% relative to si-control (*Figure* 6A). In contrast, the Cathepsin L levels and the LC3II/LC3I ratio were decreased by 52 ± 6 and 57 ± 5%, respectively. Silencing of FoxO4 increased the p62 and Cathepsin L levels as well as the LC3II/LC3I ratio in obestatin-treated myotubes by 94 ± 6, 564 ± 15 and 86 ± 3% relative to si-control, respectively (*Figure* 6A). These results demonstrate not only the role of FoxO4 in triggering the atrophy program, but also that its activity is tightly controlled by the obestatin/GPR39 system.

Post-translational regulation of FoxO1 by the obestatin/GPR39 system in dexamethasone-induced atrophy of human KM155C25 myotubes

While the obestatin/GPR39 signalling clearly controlled the FoxO4 activity by phosphorylation, altering its subcellular location, its role in regulating FoxO1 was not so clear. Nuclear/cytoplasmic shuttling of FoxO1 suggested the implication of posttranslational modifications beyond protein phosphorylation, i.e. acetylation and ubiquitination. In response to Dexa, FoxO1 was acetylated (Ac-FoxO1), and the Ac-FoxO1 level was significantly decreased by 59–76% in response to obestatin (*Figure* 6B). The acetylation status of FoxO transcription factors is generally balanced by histone acetylases and histone deacetylase (HDAC), including the NAD^+-dependent sirtuins. As shown in *Figure* 6B, FoxO1 acetylation was accompanied by the Dexa-induced phosphorylation of HDAC4 [pHDAC4(S246), 1.7-fold], but this phosphorylation was clearly decreased 29–61% in response to obestatin. In addition, Dexa treatment increased Sirt1 expression by 1.7-fold, and this expression was decreased in obestatin-treated cells (36–60% inhibition related to Dexa-treated cells; *Figure* 6B). Sirt2 was also increased 1.6-fold in response to Dexa but this expression was decreased in obestatin-treated cells (36–42% inhibition related to Dexa-treated cells; *Figure* 6B). No significant modification of Sirt3 expression was observed in any condition (*Figure* 6B). Depending on the cell/tissue type and upstream stimulus, multiple kinase families including the Ca^{2+}/CaM-dependent protein kinases (CAMKs), protein kinase D (PKDs) and AMPK can phosphorylate and regulate the localization of the class IIa HDACs.[31] The activation of PKD [pPKD/PKCμ(S916)] was up-regulated 1.7-fold in the presence of Dexa, but this action was reduced in response to obestatin (35–50% inhibition related to Dexa-treated cells; *Figure* 6B). Dexa treatment increased 2.0-fold the activation of CAMKII, estimated by the phosphorylation of CAMKII at T286 [pCAMKII(T286)], being decreased by obestatin stimulation (33–45% inhibition related to Dexa-treated cells; *Figure* 6B). Finally, activation of AMPK, estimated by the phosphorylation of AMPK at T172 [pAMPK(T172)], was increased by 2.4-fold in response to Dexa but decreased by 34–73% under obestatin stimulation (*Figure* 6A). Therefore, HDAC4 activity was regulated by interplay among PKD, CAMKII and AMPK, which suggests some mechanisms for the modulation of FoxO1 acetylation. Next, we looked for evidence of potential FoxO1-interacting proteins in control, Dexa- (1 μM) and Dexa (1 μM)/obestatin (10 nM)-treated cells. Proteins of myotube cells were immunoprecipitated with anti-FoxO1 and probed with anti-Ac-FoxO1, anti-Sirt1, anti-Sirt2, anti-Sirt3, anti-HDAC4 antibodies or anti-ubiquitin. *Figure* 7 shows that Sirt1 interacted with FoxO1, but this interaction was clearly decreased by 59 ± 1% in response to Dexa. In addition, the interaction between Sirt1 and FoxO1 was clearly increased by obestatin stimulation by 105 ± 2% as compared with Dexa-treated cells. In contrast, a significant decrease in Sirt2 was detected in Dexa-treated or obestatin-treated cells (*Figure* 7), excluding the direct involvement of this NAD^+-dependent histone deacetylase in regulating FoxO1 acetylation. No detectable changes in Sirt3 were observed after the treatments. However, we found that HDAC4 interacted with FoxO1 and this interaction was decreased by 20 ± 3% in response to Dexa, but increased by 57 ± 10% in obestatin-treated cells. We also investigated whether Dexa or obestatin signalling could modify the ubiquitination of FoxO1. Dexa treatment decreased by 54 ± 2% the ubiquitination of FOXO1 related to control levels (*Figure* 7). This effect was partly counteracted by obestatin resulting in 47 ± 3% increase in the level of ubiquitination when compared with Dexa-treated cells. Thus, obestatin/GPR39 signalling controls FoxO1 activity by altering an intricate combination of post-translational modifications, such as phosphorylation, acetylation and ubiquitination.

Figure 6 The obestatin/GPR39 system controls the proteasomal and autophagic/lysosomal systems via post-transcriptional modification of FoxO4 and FoxO1. *(A)* After transfection with specific FoxO4 siRNA, KM155C25 myotubes were treated with Dexa (1 μM) or Dexa (1 μM) + obestatin (10 nM) for 24 h. The effect of FoxO4 siRNA was evaluated on obestatin-activated signalling network, Murf1, MAFbx, p62, Cathepsin L and LC3. Protein level was expressed as fold of si-control cells (n = 3). Data were expressed as mean ± SEM. *,#,€ $P < 0.05$ vs. control values. *(B)* Immunoblot analysis of Ac-FoxO1(K259/262/271), pHDAC4(S246), pHDAC5(S259), pHDAC7(S155), HDAC4, pPKD(S744/748), pCAMKII(T286), Sirt1, pAMPK(T172) and Sirt3 in human KM155C25 myotubes under DM, DM + Dexa (1 μM, 24 h) or DM + Dexa (1 μM, 24 h) + obestatin (10–100 nM, 24 h). Immunoblots are representative of the mean value (n = 4). Data were expressed as mean ± SEM obtained from intensity scans. Data were expressed as mean ± SEM obtained from intensity scans. * $P < 0.05$ Dexa vs. DM and # $P < 0.05$ obestatin vs. Dexa.

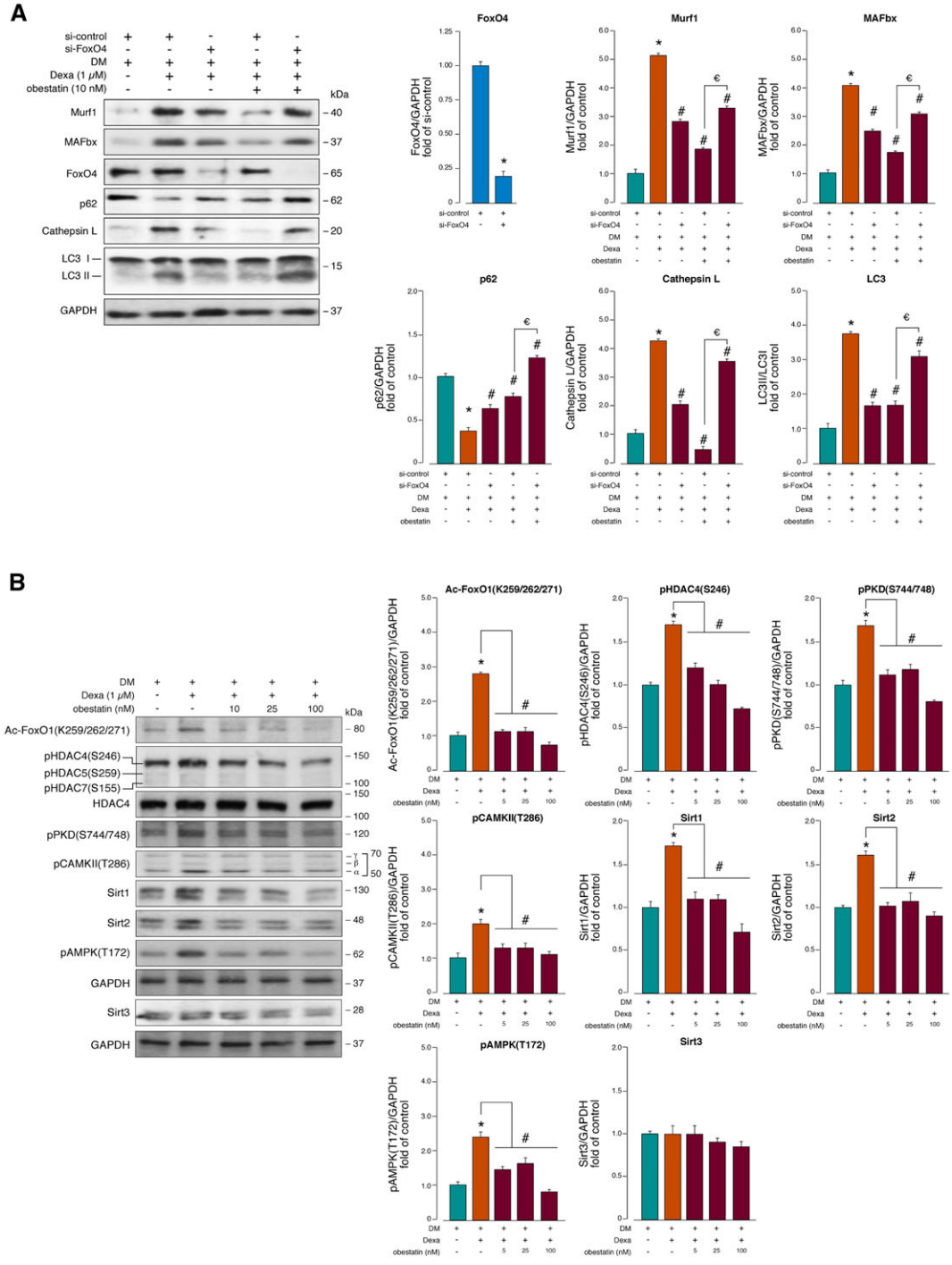

DOI: 10.1002/jcsm.12222

Figure 7 The obestatin/GPR39 system controls the FoxO1 acetylation via Sirt1 and HDAC4. (A) Co-immunoprecipitation assays used to validate the FoxO1-interacting proteins under DM, DM + Dexa (1 μM, 24 h) or DM + Dexa (1 μM, 24 h) + obestatin (10–100 nM, 24 h) stimulation. The FoxO1 complex was coimmunoprecipitated with anti-FoxO1 affinity beads and analysed by western blot using anti-Ac-FoxO1(K259/262/271), anti-Sirt1, anti-Sirt2, anti-Sirt3, anti-HDAC4, anti-ubiquitin and anti FoxO1 antibodies. Immunoblot are representative of the mean value (n = 3). Data were expressed as mean ± SEM obtained from intensity scans. Data were expressed as mean ± SEM obtained from intensity scans. * $P < 0.05$ Dexa vs. DM and # $P < 0.05$ obestatin vs. Dexa.

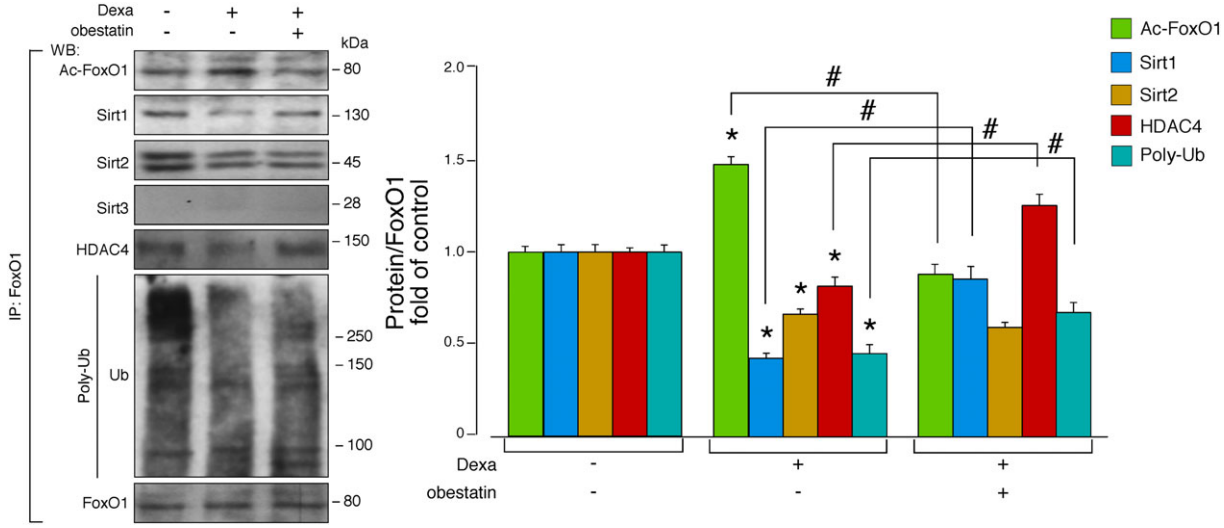

Discussion

In the present study, we have shown that obestatin specifically regulates protein synthesis, autophagy and ubiquitin–proteasome systems in a coordinated manner involving Akt-, PKD/PKCμ-, CAMKII- and AMPK-dependent mechanisms with distinct sets of effector proteins that ultimately affect FoxO transcription factors. Additionally, a specific pattern of FoxO post-translational modifications, including FoxO4 phosphorylation and FoxO1 deacetylation, is critical in the regulation of autophagy and ubiquitin–proteasome. These observations demonstrated that the obestatin/GPR39 system is able to counteract deregulations in the proteostasis, e.g. those associated to glucocorticoid-induced myotube atrophy, and to restore efficient basal homeostasis.

In the C2C12 myotubes used in this study, the regulation of the ubiquitin–proteasome machinery partly derives from the activation of the Akt pathway. Akt controls both protein degradation *via* the FoxO family transcription factors, and protein synthesis *via* mTOR.[32,33] Akt has been previously shown to phosphorylate members of the FoxO family, which keeps FOXO proteins from translocating to the nucleus.[34] Our results show that neither FoxO1 nor FoxO3 is involved in the response to obestatin *via* phosphorylation. In contrast, FoxO4 appears to be the obestatin-responsive isoform, thus suggesting an isoform specific mode of regulation. On the other hand, the implication of the mTOR pathway is demonstrated by the activation of S6 K1 and by eIF4E availability, through phosphorylation of 4E-BP1, which finally promotes protein synthesis.[4,32] Thus, the activation of the obestatin/GPR39 system results in an anti-atrophic effect as evidenced by an increase in protein content in myotube, e.g. MHC, and an increase in the size of these myotubes in the presence of atrophy-promoting Dexa. Synthesis and degradation of proteins are two processes that are intimately connected and regulated by pathways that can affect both.[32] Our report demonstrates that the activation of the obestatin/GPR39 system blocks Dexa-induced autophagy. Reduction of LC3 lipidation (LC3II) and accumulation of p62 together with a reduced Cathepsin L protein level support the hypothesis that lysosomal activity was slowed down in Dexa-treated myotubes, thereby limiting the final degradation steps of up-regulated autophagy. Thus, the obestatin/GPR39 system controls both protein synthesis and protein degradation by specific modulation of anabolism and proteasomal activity.

Although murine models sometimes can translate directly to human conditions, we show here that concerning the molecular behaviour of some key genes or key pathways, or even potentially at genome-wide level, murine myogenesis differs substantially from human myogenesis.[35–38] Although the obestatin/GPR39 system reverts Dexa-induced atrophy in human myotubes by regulating both ubiquitin–proteasome and autophagy–lysosome systems, we show here that the molecular response in the cellular mouse model C2C12 reflects only partly the mechanisms involved in human muscle cells. First, transcriptional and post-translational regulation of FoxO3 by Dexa differs between murine and human cells. Dexa activates FoxO3 at the transcriptional level in human

myotubes. Indeed, induction of FoxO3 transcripts was demonstrated to require glucocorticoid receptor-binding steroids.[39] Consistent with the stimulation of FoxO3 being a primary response to glucocorticoids, analysis of genomic DNA as well as ChIP assays revealed two functional glucocorticoid responsive elements within the FoxO3 promoter.[39] Furthermore, we provide evidence for a phosphorylation switch by which Dexa induces transcriptional activation of the FoxO3 gene but subsequently inactivates the corresponding protein by site-specific phosphorylation, i.e. T32, S381 and S321. Thus, glucocorticoid appears to exert a dual action in activating FoxO3 target gene expression by combining transcriptional and post-translational levels of regulation. Recent evidence indicated that FoxO3 transcription factor is activated in response to metabolic stress, characterized by low intracellular energy and high glucocorticoid levels.[40–43] Under these conditions, FoxO3 is activated on the transcriptional level and phosphorylated by AMPK. This results in an increased transcription of the FoxO3 target gene Liver Kinase B1 (LKB1), which in turn can phosphorylate and thereby activate AMPK.[39] Once activated, AMPK switches off anabolic pathways while simultaneously activating catabolic pathways, which result in the production of ATP.[44] When cellular energy levels are restored, AMPK is then allosterically inactivated by ATP.[45,46] Under such conditions, the serum and glucocorticoid-inducible kinase 1 (SGK-1) phosphorylates FoxO3 at T32, inactivating its transcriptional activity.[39] Furthermore, the fact that the induction of FoxO3 transcripts was enhanced by AMPK activation under Dexa treatment, but inhibited by the obestatin-related Akt signalling, suggests that Akt and the AMPK pathways can have opposite biological effects. While the obestatin-related Akt pathway stimulates the anabolic process, the AMPK pathway promotes catabolic process. FoxO3 is one of the intersections between the two pathways, being post-translationally inhibited by downstream effectors of the Akt pathway and post-translationally regulated by AMPK. Thus, the AMPK signalling pathway may coordinate a series of transcriptional and post-transcriptional changes that allow cells to adapt to changes in the energy status. Second, FoxO1 activity is not only regulated by phosphorylation at Akt-phosphorylation site S256,[47–49] but also the acetylation of FoxO1 is involved in human myotubes. Akt-phosphorylation site S256 is a requisite to promote ubiquitination and degradation of FoxO1.[50] Additionally, the acetylation status of FoxO1 is associated to specific dephosphorylation of class II HDAC4 on a series of conserved serine residues. Indeed, HDAC phosphorylation provides docking sites for the 14-3-3 chaperone protein leading to nuclear export and inactivation of HDACs.[51,52] The increase HDAC4 activity occurred together with significant changes in the activation of PKD/PKCμ and CAMKII, enzymes known to regulate class II HDAC activation via phosphorylation.[53–56] This is further supported by results of immunoprecipitation assays that demonstrate that HDAC4 interacts with FoxO1, and that this interaction is clearly decreased in response to Dexa. We also observed an increased interaction between FoxO1 and Sirt1, and not Sirt2, under obestatin stimulation. Taking into account the role of acetylation on FoxO1 activity on autophagy,[57–62] FoxO1 could function in eliciting autophagy in response to Dexa by directly binding to the promoter region of autophagic genes[63,64] or by specific interaction with Atg7, an E1-following protein, to influence the autophagic process.[62] On the other hand, the lack of Akt-specific phosphorylation of FoxO1 at S256 prevents its degradation.[50] Thus, we propose that the obestatin/GPR39 signalling has exerted its specific function by reducing FoxO1 activity by deacetylation and phosphorylation. Deacetylation of FoxO1 occurs as a result of its association to Sirt1 and HDAC4, and the deacetylated FoxO1 fails to induce the autophagic process. Obestatin-related Akt signalling promotes the ubiquitin-dependent degradation via FoxO1 phosphorylation, thereby inhibiting its transcriptional function. This is further supported by our results showing that obestatin can increase the ubiquitination status of FoxO1, and thus accelerate its degradation. Third, the Dexa-induced expression pattern of myogenin is different between mouse and human myotubes. Myogenin plays a dual role as both a regulator of muscle development and an inducer of neurogenic atrophy by directly activating the expression of MuRF1 and MAFbx in mice.[16,65] These contrasting activities reflect differential modulation by signalling pathways that enable myogenin to regulate distinct sets of target genes.[65] Although myogenin was up-regulated in C2C12 myotubes following Dexa treatment, at no time, this transcription factor did show an increase in human myotubes. This might be ascribed to differences in kinetics of myogenin expression between cellular models. The precise mechanisms underlying this phenomenon are unclear; however, the fact that MuRF1 and MAFbx are down-regulated under obestatin treatment in the absence of myogenin up-regulation appears to exclude its implication as inducer of the E3 ubiquitin ligases in glucocorticoid-induced atrophy. In this regard, myogenin is not induced in response to other forms of atrophy such as cancer, fasting or diabetes.[66,67] Together, these findings highlight the existence of fundamental differences between the regulatory circuitry in human and mouse muscle wasting and their modulation. Further experimentation will be required to fully elucidate the functional consequences of these differences.

Obestatin/GPR39 system arises as one of the autocrine systems for coordinating muscle growth, enhancing muscle repair and increasing muscle mass through regulatory role on proliferation, differentiation and hypertrophy of muscle cells.[24–26] If one adds to this a role in regulating muscle atrophy through regulation of ubiquitin E3-ligases expression and autophagy, this system displays clear functional similarities with the IGF and/or insulin signalling, but acts using distinct receptors and signalling pathways. The major

Figure 8 Restoration of anabolic conditions by obestatin/GPR39 signalling in Dexa-induced skeletal muscle cell atrophy model. Schematic model of mutual crosstalk between catabolic processes associated to GR activation and anabolic processes activated by obestatin in human skeletal muscle cells.

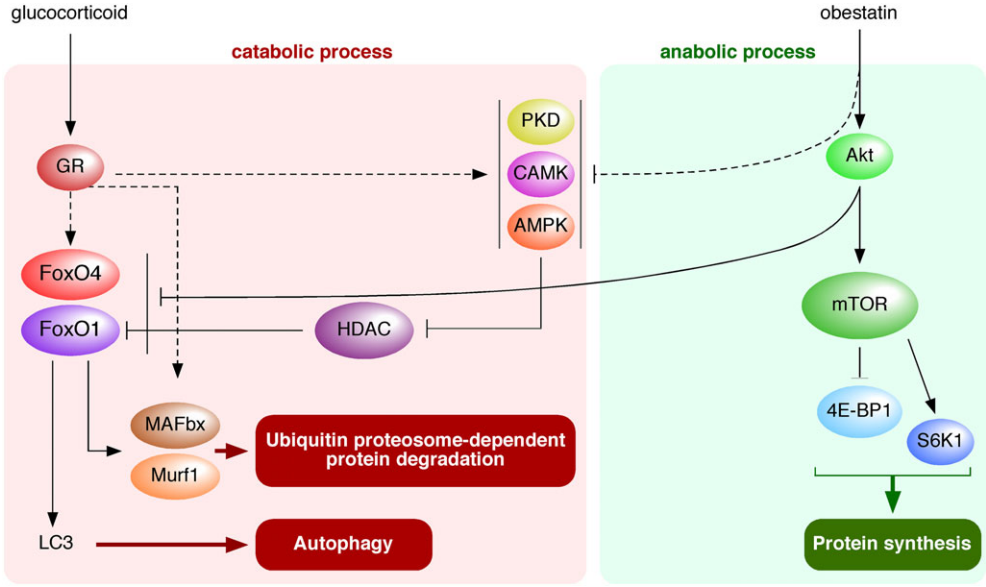

findings in this work have been the identification of key anti-atrophic signalling nodes in humans, in particular FoxO4 and FoxO1, in response to obestatin. It is worth underlining that, siRNA targeting FoxO4 suppress the ability of obestatin to regulate E3 ubiquitin ligases and autophagy during glucocorticoid treatment. Furthermore, FoxO1 is regulated by post-translational modifications, for example acetylation/deacetylation and ubiquitination. Interestingly, the obestatin action was not due to an effect on the FoxO3, the most critical factor for the atrophy program.[6,12,15] Indeed, we provide functional evidence for a FoxO3 phosphorylation switch that explains how glucocorticoids, *per se*, regulate transcriptional activation of the gene but subsequently inactivate the corresponding protein by site-specific phosphorylation and nuclear export. Therefore, FoxO4 and FoxO1 are both required for the optimal regulation of the proteostasis in response to the obestatin/GPR39 system, at least during glucocorticoid-induced atrophy.

In summary, our results demonstrate that the activation of obestatin/GPR39 system impaired proteostasis via specific inactivation of FoxO4 and FoxO1 and efficiently counteracts the catabolic processes provoked by glucocorticoids, as shown in *Figure* 8. Notably, Akt/mTOR activation combined with PKD/CAMKII/AMPK inactivation by the obestatin signalling is required to inhibit FoxO-dependent atrogenes and autophagy in human muscle cells. This crosstalk between GR and the obestatin/GPR39 signalling is a coordinated interaction between an anabolic signal and the catabolic machinery. Modulation of the activity of this system may represent a new strategy to ameliorate the debilitating effects of the muscle atrophic response to glucocorticoids.

Acknowledgements

Marta Picado Barreiro is greatly acknowledged for assistance with the confocal microscope experiments. The platform for immortalization of human cells of the Center of Research in Myology is acknowledged, particularly K. Mamchaoui, as well as the MYOBANK-AFM in the Myology Institute (code BB-0033-00012). The authors certify that they comply with the ethical guidelines for authorship and publishing of the Journal of Cachexia, Sarcopenia and Muscle.[68]

This work was supported by grants from Instituto de Salud Carlos III in co-financing with FEDER (ISCIII-FEDER; MINECO, Spain; PI15/01537) and Programa PRIS (SERGAS in co-financing with FEDER). The work of JP Camiña and Y Pazos are funded by the ISCIII and SERGAS through a research-staff stabilization contract. Xunta de Galicia funds J González-Sánchez through a pre-doctorate research scholarship. IDIS funds T Cid-Diaz through a pre-doctorate research scholarship.

Online supplementary material

Additional Supporting Information may be found online in the supporting information tab for this article.

Figure S1. Activation of the obestatin/GPR39 system regulates the C25 myotube growth under Dexa-treatment. (A) *Left panel*, immunofluorescence detection of MHC in C25 myotube cells after stimulation under differentiation

medium (DM), DM + Dexa (1 μM, 24 h) + obestatin (10 nM, 24 h) or DM + Dexa (1 μM, 24 h), applied at day 7 post-differentiation. DAPI was used to identify the cell nucleus. *Right panel* corresponds to myotube area (μm^2) assessment for the different treatments (n = 10 per group). Data were expressed as mean ± SEM. (B) Immunoblot analysis of Murf1, MAFbx, pFoxO3a(T32), pFoxO1(T24) and pFoxO4(T28) in C25 myotubes under DM, DM + Dexa (1 μM, 24 h) + obestatin (10 nM, 24 h) or DM + Dexa (1 μM, 24 h). Immunoblots are representative of the mean value. Data were expressed as mean ± SEM obtained from intensity scans. In A-B * $P < 0.05$ Dexa + obestatin or Dexa vs. control values (DM); # $P < 0.05$ Dexa + obestatin vs. Dexa values.

Figure S2. β-Arrestins determine Akt signalling pathway associated to the obestatin/GPR39 system in human KM155C25 myotubes. After transfection with specific β-arrestin 1 or 2 siRNAs, KM155C25 myotubes were treated with obestatin (10nM) for 10min. The effect of β-arrestin 1 or 2 siRNAs was evaluated on obestatin-activated signalling network, pAkt(S473), pFoxO3a(T32), pFoxO1(T24), pFoxO4(T28), pFoxO1(S256) and pFoxO3a(S318/321). Protein level was expressed as fold of si-control cells (n = 3). Data were expressed as mean ± SEM. * P *< 0.05 vs. control si-control values; # $P < 0.05$ si-ßarrestin + obestatin vs. si-control + obestatin values.

Table S1. Supporting Information.

Conflict of interest

The authors declare that they have no conflicts of interest.

References

1. Hoffman EP, Nader GA. Balancing muscle hypertrophy and atrophy. *Nat Med* 2004;**10**:584–585.
2. Bodine SC, Baehr LM. Skeletal muscle atrophy and the E3 ubiquitin ligases MuRF1 and MAFbx/atrogin-1. *Am J Physiol Endocrinol Metab* 2014;**307**: E469–E484.
3. Miyazaki M, Esser KA. Cellular mechanisms regulating protein synthesis and skeletal muscle hypertrophy in animals. *J Appl Physiol* 2009;**106**:1367–1373.
4. Laplante M, Sabatini DM. mTOR signaling in growth control and disease. *Cell* 2012;**149**:274–293.
5. Sandri M. Signaling in muscle atrophy and hypertrophy. *Physiology (Bethesda)* 2008;**23**:160–170.
6. Mammucari C, Milan G, Romanello V, Masiero E, Rudolf R, Del Piccolo P, et al. FoxO3 controls autophagy in skeletal muscle in vivo. *Cell Metab* 2007;**6**:458–471.
7. Sandri M. Autophagy in skeletal muscle. *FEBS Lett* 2010;**584**:1411–1416.
8. Glass DJ. Signalling pathways that mediate skeletal muscle hypertrophy and atrophy. *Nat Cell Biol* 2003;**5**:87–90.
9. Sandri M, Sandri C, Gilbert A, Skurk C, Calabria E, Picard A, et al. Foxo transcription factors induce the atrophy-related ubiquitin ligase atrogin-1 and cause skeletal muscle atrophy. *Cell* 2004;**117**:399–412.
10. Mizushima N, Levine B, Cuervo AM, Klionsky DJ. Autophagy fights disease through cellular self-digestion. *Nature* 2008;**451**:1069–1075.
11. Webb AE, Brunet A. FOXO transcription factors: key regulators of cellular quality control. *Trends Biochem Sci* 2014;**39**:159–169.
12. Zhao J, Brault JJ, Schild A, Cao P, Sandri M, Schiaffino S, et al. FoxO3 coordinately activates protein degradation by the autophagic/lysosomal and proteasomal pathways in atrophying muscle cells. *Cell Metab* 2007;**6**:472–483.
13. Xu J, Li R, Workeneh B, Dong Y, Wang X, Hu Z. Transcription factor FoxO1, the dominant mediator of muscle wasting in chronic kidney disease, is inhibited by microRNA-486. *Kidney Int* 2012;**82**:401–411.
14. Yamazaki Y, Kamei Y, Sugita S, Akaike F, Kanai S, Miura S, et al. The cathepsin L gene is a direct target of FOXO1 in skeletal muscle. *Biochem J* 2010;**427**:171–178.
15. Milan G, Romanello V, Pescatore F, Armani A, Paik JH, Frasson L, et al. Regulation of autophagy and the ubiquitin–proteasome system by the FoxO transcriptional network during muscle atrophy. *Nat Commun* 2015;**6**:6670.
16. Moressi V, Williams AH, Meadows E, Flynn JM, Potthoff MJ, McAnally J, et al. Myogenin and class II HDACs control neurogenic muscle atrophy by inducing E3 ubiquitin ligases. *Cell* 2010;**143**:35–45.
17. Meijsing SH, Pufall MA, So AY, Bates DL, Chen L, Yamamoto KR. DNA binding site sequence directs glucocorticoid receptor structure and activity. *Science* 2009;**324**:407–410.
18. Munck A, Holbrook NJ. Glucocorticoid-receptor complexes in rat thymus cells. Rapid kinetic behavior and a cyclic model. *J Biol Chem* 1984;**259**:820–831.
19. Menconi M, Fareed M, O'Neal P, Poylin V, Wei W, Hasselgren PO. Role of glucocorticoids in the molecular regulation of muscle wasting. *Crit Care Med* 2007;**35**: S602–S608.
20. Schakman O, Kalista S, Bertrand L, Lause P, Verniers J, Ketelslegers JM, Thissen JP. Role of Akt/GSK-3beta/beta-catenin transduction pathway in the muscle anti-atrophy action of insulin-like growth factor-I in glucocorticoid-treated rats. *Endocrinology* 2008;**149**:3900–3908.
21. Hu Z, Wang H, Lee IH, Du J, Mitch WE. Endogenous glucocorticoids and impaired insulin signaling are both required to stimulate muscle wasting under pathophysiological conditions in mice. *J Clin Invest* 2009;**119**:3059–3069.
22. Stitt TN, Drujan D, Clarke BA, Panaro F, Timofeyva Y, Kline WO, et al. The IGF-1/PI3K/Akt pathway prevents expression of muscle atrophy-induced ubiquitin ligases by inhibiting FOXO transcription factors. *Mol Cell* 2004;**14**:395–403.
23. Shimizu N, Yoshikawa N, Ito N, Maruyama T, Suzuki Y, Takeda S, et al. Crosstalk between glucocorticoid receptor and nutritional sensor mTOR in skeletal muscle. *Cell Metab* 2011;**13**:170–182.
24. Gurriaran-Rodriguez U, Santos-Zas I, Al-Massadi O, Mosteiro CS, Beiroa D, Nogueiras R, et al. The obestatin/GPR39 system is up-regulated by muscle injury and functions as an autocrine regenerative system. *J Biol Chem* 2012;**287**:38379–38389.
25. Gurriaran-Rodriguez U, Santos-Zas I, González-Sánchez J, Beiroa D, Moresi V, Mosteiro C, et al. The action of obestatin in skeletal muscle repair: stem cell expansion, muscle growth, and microenvironment remodeling. *Mol Theraphy* 2015;**23**:1003–1021.
26. Santos-Zas I, Gurriarán-Rodríguez U, Cid-Díaz T, Figueroa G, González-Sánchez J, Bouzo-Lorenzo M, et al. β-Arrestin scaffolds and signaling elements essential for the obestatin/GPR39 system that determine the myogenic program in human myoblast cells. *Cell Mol Life Sci* 2016;**73**:617–635.
27. Bodine SC, Stitt TN, Gonzalez M, Kline WO, Stover GL, Bauerlein R, et al. Akt/mTOR

pathway is a crucial regulator of skeletal muscle hypertrophy and can prevent muscle atrophy in vivo. *Nat Cell Biol* 2001;**3**:1014–1019.
28. Latres E, Amini AR, Amini AA, Griffiths J, Martin FJ, Wei Y, et al. Insulin-like growth factor-1 (IGF-1) inversely regulates atrophy-induced genes via the phosphatidylinositol 3-kinase/Akt/mammalian target of rapamycin (PI3K/Akt/mTOR) pathway. *J Biol Chem* 2005;**280**:2737–2744.
29. Mamchaoui K, Trollet C, Bigot A, Negroni E, Chaouch S, Wolff A, et al. Immortalized pathological human myoblasts: towards a universal tool for the study of neuromuscular disorders. *Skelet Muscle* 2011;**1**:34.
30. Thorley M, Duguez S, Mazza EM, Valsoni S, Bigot A, Mamchaoui K, Harmon B, Voit T, Mouly V, Duddy W. Skeletal muscle characteristics are preserved in hTERT/cdk4 human myogenic cell lines. *Skelet Muscle* 2016;**6**:43.
31. Mihaylova MM, Shaw RJ. Metabolic reprogramming by class I and II histone deacetylases. *Trends Endocrinol Metab* 2013;**24**:48–57.
32. Bonaldo P, Sandri M. Cellular and molecular mechanisms of muscle atrophy. *Dis Model Mech* 2013;**6**:25–39.
33. Schakman O, Kalista S, Barbé C, Loumaye A, Thissen JP. Glucocorticoid-induced skeletal muscle atrophy. *Int J Biochem Cell Biol* 2013;**45**:2163–2172.
34. Calnan DR, Brunet A. The FoxO code. *Oncogene* 2008;**27**:2276–2288.
35. Bachrach E, Li S, Perez AL, Schienda J, Liadaki K, Volinski J, Flint A, Chamberlain J, Kunkel LM. Systemic delivery of human microdystrophin to regenerating mouse dystrophic muscle by muscle progenitor cells. *Proc Natl Acad Sci U S A* 2004;**101**:3581–3586.
36. Bareja A, Holt JA, Luo G, Chang C, Lin J, Hinken AC, et al. Human and mouse skeletal muscle stem cells, convergent and divergent mechanisms of myogenesis. *PLoS One* 2014;**9**:e90398.
37. Boldrin L, Muntoni F, Morgan JE. Are human and mouse satellite cells really the same? *J Histochem Cytochem* 2010;**58**:941–955.
38. Boldrin L, Neal A, Zammit PS, Muntoni F, Morgan JE. Donor satellite cell engraftment is significantly augmented when the host niche is preserved and endogenous satellite cells are incapacitated. *Stem Cells* 2012;**30**:1971–1984.
39. Lützner N, Kalbacher H, Krones-Herzig A, Rösl F. FOXO3 is a glucocorticoid receptor target and regulates LKB1 and its own expression based on cellular AMP levels via a positive autoregulatory loop. *PLoS One* 2012;**7**:e42166.
40. Foss ML, Barnard RJ, Tipton CM. Free 11-hydroxycorticosteroid levels in working dogs as affected by exercise training. *Endocrinology* 1971;**89**:96–104.
41. Few JD. Effect of exercise on the secretion and metabolism of cortisol in man. *J Endocrinol* 1974;**62**:341–353.
42. Sellers TL, Jaussi AW, Yang HT, Heninger RW, Winder WW. Effect of the exercise-induced increase in glucocorticoids on endurance in the rat. *J Appl Physiol* 1988;**65**:173–178.
43. Wasserman DH. Regulation of glucose fluxes during exercise in the postabsorptive state. *Annu Rev Physiol* 1995;**57**:191–218.
44. Hardie DG. AMP-activated/SNF1 protein kinases: conserved guardians of cellular energy. *Nat Rev Mol Cell Biol* 2007;**8**:774–785.
45. Yeh LA, Lee KH, Kim KH. Regulation of rat liver acetyl-CoA carboxylase. Regulation of phosphorylation and inactivation of acetyl-CoA carboxylase by the adenylate energy charge. *J Biol Chem* 1980;**255**:2308–2314.
46. Scott JW, Hawley SA, Green KA, Anis M, Stewart G, et al. CBS domains form energy-sensing modules whose binding of adenosine ligands is disrupted by disease mutations. *J Clin Invest* 2004;**113**:274–284.
47. Aoki M, Jiang H, Vogt PK. Proteasomal degradation of the FoxO1 transcriptional regulator in cells transformed by the P3k and Akt oncoproteins. *Proc Natl Acad Sci U S A* 2004;**101**:13613–13617.
48. Plas DR, Thompson CB. Akt activation promotes degradation of tuberin and FOXO3a via the proteasome. *J Biol Chem* 2003;**278**:12361–12366.
49. Matsuzaki H, Daitoku H, Hatta M, Tanaka K, Fukamizu A. Insulin-induced phosphorylation of FKHR (Foxo1) targets to proteasomal degradation. *Proc Natl Acad Sci U S A* 2003;**100**:11285–11290.
50. Huang H, Regan KM, Wang F, Wang D, Smith DI, van Deursen JM, Tindall DJ. Skp2 inhibits FOXO1 in tumor suppression through ubiquitin-mediated degradation. *Proc Natl Acad Sci U S A* 2005;**102**:1649–1654.
51. McKinsey TA, Zhang CL, Lu J, Olson EN. Signal-dependent nuclear export of a histone deacetylase regulates muscle differentiation. *Nature* 2000;**408**:106–111.
52. McKinsey TA, Zhang CL, Olson EN. Signaling chromatin to make muscle. Curr Opin Cell Biol. 2002; **14**: 763-772.5264 Potthoff MJ, Olson EN. MEF2: a central regulator of diverse developmental programs. *Development* 2007;**134**:4131–4140.
53. Vega RB, Harrison BC, Meadows E, Roberts CR, Papst PJ, Olson EN. Protein kinases C and D mediate agonist-dependent cardiac hypertrophy through nuclear export of histone deacetylase 5. *Mol Cell Biol* 2004;**24**:8374–8385.
54. Dequiedt F, Van LJ, Lecomte E, Van D, Seufferlein VT, Vandenheede JR. Phosphorylation of histone deacetylase 7 by protein kinase D mediates T cell receptor-induced Nur77 expression and apoptosis. *J Exp Med* 2005;**201**:793–804.
55. Parra M, Kasler H, McKinsey TA, Olson EN, Verdin E. Protein kinase D1 phosphorylates HDAC7 and induces its nuclear export after T-cell receptor activation. *J Biol Chem* 2005;**280**:13762–13770.
56. Backs J, Song K, Bezprozvannaya S, Chang S, Olson EN. CaM kinase II selectively signals to histone deacetylase 4 during cardiomyocyte hypertrophy. *J Clin Invest* 2006;**116**:1853–1864.
57. Brunet A, Sweeney LB, Sturgill JF, Chua KF, Greer PL, Lin Y, et al. Stress-dependent regulation of FOXO transcription factors by the SIRT1 deacetylase. *Science* 2004;**303**:2011–2015.
58. Motta MC, Divecha N, Lemieux M, Kamel C, Chen D, Gu W, et al. Mammalian SIRT1 represses forkhead transcription factors. *Cell* 2004;**116**:551–563.
59. Daitoku H, Hatta M, Matsuzaki H, Aratani S, Ohshima T, Miyagishi M, et al. Silent information regulator 2 potentiates Foxo1-mediated transcription through its deacetylase activity. *Proc Natl Acad Sci U S A* 2004;**101**:10042–10047.
60. Jing E, Gesta S, Kahn CR. SIRT2 regulates adipocyte differentiation through FoxO1 acetylation/deacetylation. *Cell Metab* 2007;**6**:105–114.
61. Lee IH, Cao L, Mostoslavsky R, Lombard DB, Liu J, Bruns NE, et al. A role for the NAD-dependent deacetylase Sirt1 in the regulation of autophagy. *Proc Natl Acad Sci U S A* 2008;**105**:3374–3379.
62. Zhao Y, Yang J, Liao W, Liu X, Zhang H, Wang S, et al. Cytosolic FoxO1 is essential for the induction of autophagy and tumour suppressor activity. *Nat Cell Biol* 2010;**12**:665–675.
63. Liu J, Bi X, Chen T, Zhang Q, Wang SX, Chiu JJ, et al. Shear stress regulates endothelial cell autophagy via redox regulation and Sirt1 expression. *Cell Death Dis* 2015;**6**: e1827.
64. Qiang L, Banks AS, Accili D. Uncoupling of acetylation from phosphorylation regulates FoxO1 function independent of its subcellular localization. *J Biol Chem* 2010;**285**:27396–27401.
65. Tang H, Goldman D. Activity-dependent gene regulation in skeletal muscle is mediated by a histone deacetylase (HDAC)-Dach2-myogenin signal transduction cascade. *Proc Natl Acad Sci U S A* 2006;**103**:16977–16982.
66. Lecker SH, Jagoe RT, Gilbert A, Gomes M, Baracos V, Bailey J, Price SR, Mitch WE, Goldberg AL. Multiple types of skeletal muscle atrophy involve a common program of changes in gene expression. *FASEB J* 2004;**18**:39–51.
67. Sacheck JM, Hyatt JP, Raffaello A, Jagoe RT, Roy RR, Edgerton VR, Lecker SH, Goldberg AL. Rapid disuse and denervation atrophy involve transcriptional changes similar to those of muscle wasting during systemic diseases. *FASEB J* 2007;**21**:140–155.
68. von Haehling S, Morley JE, Coats AJS, Anker SD. Ethical guidelines for authorship and publishing in the Journal of Cachexia, Sarcopenia and Muscle. *J Cachexia Sarcopenia Muscle* 2015;**4**:315–316.